Supporting Information for the manuscript

A two-component adhesive: Tau fibrils arise from a combination of a well-defined motif and conformationally flexible interactions

Shengqi Xiang[1], Natalia Kulminskaya[1], Birgit Habenstein[1,2], Jacek Biernat[3,4], Katharina Tepper[3,4], Maria Paulat[1], Christian Griesinger[1], Stefan Becker[1], Adam Lange[1,5,6], Eckhard Mandelkow[3,4,7], and Rasmus Linser[1,8]*

1) Max-Planck Institute for Biophysical Chemistry, Department NMR-Based Structural Biology, Am Fassberg 11, 37077 Göttingen, Germany
2) Université de Bordeaux/CBMN UMR5248, Institut Européen de Chimie et Biologie (IECB), 2 rue Robert Escarpit, 33600 Pessac (France).
3) DZNE, German Center for Neurodegenerative Diseases, Ludwig-Erhard-Allee 2, 53175 Bonn, Germany
4) CAESAR Research Center, Ludwig-Erhard-Allee 2, 53175 Bonn, Germany
5) Humboldt-Universität zu Berlin, Institut für Biologie, Invalidenstrasse 110, 10115 Berlin, Germany
6) Leibniz-Institut für Molekulare Pharmakologie (FMP), Department of Molecular Biophysics, Robert-Rössle-Strasse 10, 13125 Berlin, Germany
7) Max-Planck-Institute for Metabolism Research, Hamburg Outstation, c/o DESY, Notkestrasse 85, 22607 Hamburg.
8) Ludwig-Maximilians-University Munich, Department Chemistry and Pharmacy, Butenandtstr. 5-13, 81377 Munich, Germany

**Corresponding author:*
Prof. Dr. Rasmus Linser, Ludwig-Maximilians-University Munich, Department Chemistry and Pharmacy, Butenandtstr. 5-13, 81377 Munich, Germany, Tel. +4989218077652,
Email: rasmus.linser@lmu.de

Experimental details

PHF assembly was performed following a published protocol[1] with modifications. Briefly, the purified protein was dialyzed against 20mM BES buffer, pH 7.4, 25 mM NaCl. The protein concentration was adjusted to 2.8 mM and assembly was performed with a protein:heparin (MW ~20.000 Da) ratio of 4:1 for 4 days at 37°C. The reaction mixture was centrifuged at 160.000 × g, washed once with sodium phosphate buffer, pH 6.8, 0.1 % NaN_3 and analyzed by negative-stain EM. The final PHF samples were transferred into 4.0 and 1.3 mm NMR rotors and spun at up to 11 and 56 kHz, respectively. Effective sample temperatures were dependent on the experiment and are specified individually in the text. Traditional approaches at 11 kHz MAS employed amounts of ca. 40 mg at 850 MHz ^{1}H Larmor frequency using a Bruker Avance III spectrometer. We recorded standard 2D NCA, 2D NCO and 2D NcaCB-DREAM as well as 3D NCACX and NCOCX spectra in addition to 2D PDSD carbon-carbon correlations, using high-power SPINAL-64 decoupling of approximately 80 kHz. Proton-detected experiments were recorded on 1 mg of the same sample at 800 MHz ^{1}H Larmor frequency again using a Bruker Avance III spectrometer. Assignment experiments were mostly based on hCACONH/hCOCANH experiments using four-dimensional chemical-shift encoding (see main text Fig. 2B and Supplementary Fig. 1).[2,3] In addition, an hNcocaNH experiment yielded complementary sequential-connectivity information and was used for confirmation.[4] An hCBCANH experiment was recorded for residue type characterization. Altogether, this characterization enabled highly unambiguous sequential assignment of H^N, N^H, Cα, and Cβ shifts. Assignments were done using the CCPNmr suite[5] and the Sparky program.[6] For readout of ^{15}N line widths, line shape fitting was applied as implemented in Bruker topspin.

Table S1. The carbon-detected experiments were carried out using the parameters of each dipolar-transfer step as listed in the following table:

Transfer steps	Contact time(μs)	Pulses
H->C	700	H:67 kHz (80-100 % ramp on H)/C:50 kHz
H->N	350	H:47kHz (80-100 % ramp on H) /N:34.7 kHz
N-> Cα	3000	N:4.4kHz/Cα:49.2kHz (80-100 % ramp on Cβ/Cα)
Cα -> Cβ	1500	DREAM, average power 5kHz

A water-edited experiment was implemented as described before[1,7] with a T_2 filter of 5 ms and a diffusion time of 12 ms. The site specificity obtained for the fully protonated sample is slightly broadened due to spin diffusion. In NCA and NCACB experiments, the indirect evolution time of ^{15}N chemical shifts was set to 18 ms, and in water-edited experiments, the ^{15}N dimension was evolved up to 15 ms. In all ^{13}C-detected experiments, the acquisition time of the direct dimension was 14 ms.
Experimental peculiarities of the proton-detected experiments were applied as described in detail before.[2] These approaches are based on higher-dimensionality, proton-detected spectra[3] using dipolar mechanisms for all magnetization transfers[8] and fast MAS.
Sample C used for chemical-shift comparison was characterized using ^{13}C-based 2D and 3D approaches only at the time, which entail slightly lower assignment fidelity than the 4D assignment used in the latest sample D subjected to proton-detected 4D methods.

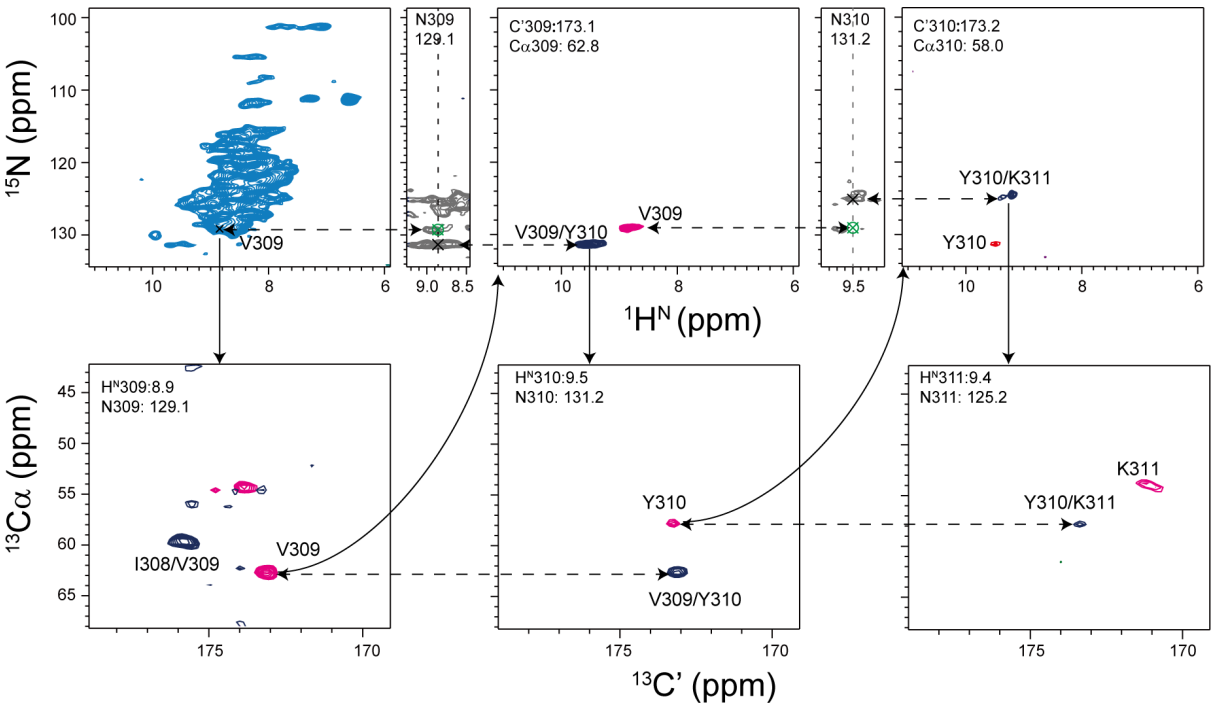

Fig. 1: Backbone walk based on 4D hCOCANH (magenta) and hCACONH (dark blue) and 3D hNcacoNH (gray) for unambiguous assignments of the heterogeneously broadened preparation (employed for sample D). Assignments were obtained by this strategy on a 1-mg sample at 56 kHz spinning and 800 MHz ^{1}H Larmor frequency. The upper left panel shows an H/N correlation for overview. The green crosses mark the diagonal position in the hNcacoNH spectra.

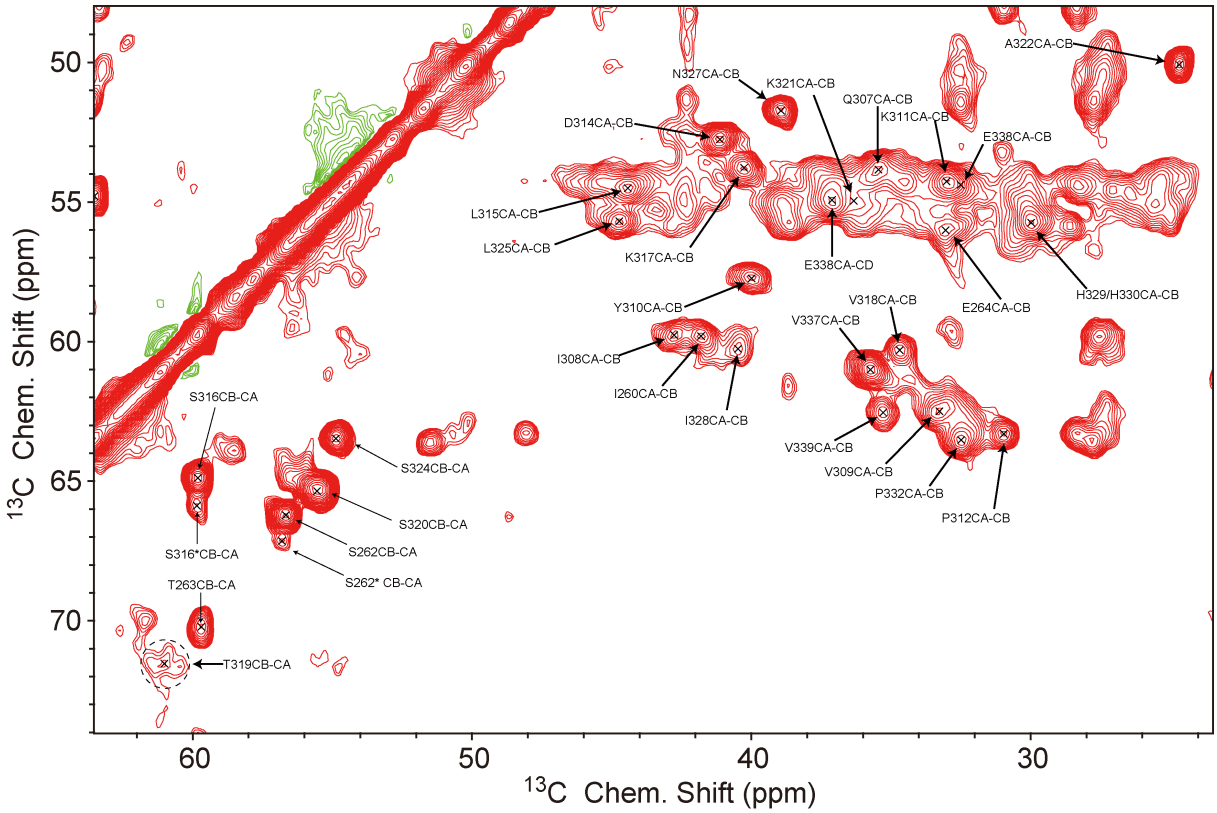

Fig. 2: ^{13}C-^{13}C-PDSD of sample D with resonance assignments. All peak assignments were transferred from the combination of 4D HNCACO/HNCOCA, 3D HNCACONH, 3D CBCANH, 3D NCACX, and 3D NCOCX spectra. Experimental parameters are given on SI page 1.

Chemical shifts

Chemical shifts employed in the quantitative comparison were partly obtained newly in this study (samples C and D, see shifts below) and partly taken from the two previous solid-state NMR studies on Tau (sample A: Andronesi et al., and sample B: Daebel et al.).[1,9]

Chemical-shift changes are minor between proton-detected spectra, obtained at 33 °C due to frictional heating at fast MAS, and traditional, ^{13}C-detected spectra, obtained at 5, 11, and 26 °C (see main text Fig. 3D and Supplementary Fig. 9). Except proton and CO, all chemical shift values are given as obtained from ^{13}C-detected spectra at 11°C.

Table S2: Chemical Shifts of Sample *C*
(obtained using traditional 3D ^{13}C-detected experiments as described earlier[1,9] only, implying reduced fidelity compared with the latest preparation, sample D)

Num	Res	N	CO	CA	CB
306	V	-	-	61.0	34.8
307	Q	-	-	54.5	32.9
308	I	123.3	174.4	59.8	42.2
309	V	127.4	-	61.5	34.2
310	Y	131.2	-	57.6	40.3
311	K	124.9	-	54.4	35.4
312	P	134.2	171.0	63.9	32.7
313	V	118.8	-	61.2	35.3
314	D	127.9	174.6	53.4	41.8
315	L	128.3	177.5	54.6	43.4
316	S	119.7	177.6	59.9	65.5
317	K	116.0	174.4	55.2	37.1
318	V	125.4	-	61.3	33.6
319	T	126.5	174.5	61.4	70.4
320	S	122.7	173.1	56.8	65.1
321	K	125.2	-	54.7	36.6
322	A	126.4	176.0	50.6	20.1
323	G	105.5	174.1	46.3	-
324	S	120.4	171.9	58.4	67.5
325	L	117.2	176.4	55.5	45.6
326	G	105.9	-	44.3	-
327	N	118.1	-	53.3	40.4
328	I	120.5	-	59.7	39.0
329	H	124.3	-	54.8	-
330	H	116.2	-	53.4	31.4
331	K	-	-	56.6	33.3
332	P	137.1	177.5	62.9	32.7
333	G	109.7	-	45.1	-
334	G	109.8	-	44.8	-
335	G	108.7	-	43.9	-
336	Q	119.8	-	55.0	31.9
337	V	123.7	-	60.7	35.2
338	E	126.4	-	54.6	34.1
339	V	-	-	61.1	35.9

Table S3: Chemical Shifts of Sample *D:*

Num	Res	H	N	CO	CA	CB
260	I	8.6	123.7	176.8	59.7	41.8
261	G	8.7	118.0	173.2	48.6	-
262	S	8.1	116.6	173.6	56.9	66.3
263	T	8.3	112.0	175.8	60.0	70.7
264	E	8.0	122.0	175.5	56.0	33.1
307	Q	8.5	124.5	174.0	54.0	35.2
308	I	8.6	124.7	175.7	59.8	42.7
309	V	8.9	128.7	173.4	62.3	33.5
310	Y	9.5	131.5	173.5	57.7	40.0
311	K	9.4	124.4	171.0	54.2	33.0
312	P	-	-	176.2	63.4	31.0
313	V	8.4	120.0	175.7	60.9	35.7
314	D	8.5	127.2	173.7	52.8	41.1
315	L	10.0	130.1	176.9	54.7	44.4
316	S	8.1	119.0	174.1	59.8	65.0
317	K	8.2	118.5	174.8	53.9	40.3
318	V	7.7	121.5	175.3	60.3	34.6
319	T	8.3	124.7	174.0	61.2	70.9
320	S	8.4	116.8	173.7	55.4	65.3
321	K	8.7	125.8	174.3	55.0	36.5
322	A	8.7	122.8	175.5	50.1	24.6
323	G	8.3	105.8	171.2	44.8	-
324	S	8.8	119.9	174.4	54.8	63.4
325	L	8.3	127.3	177.0	55.8	44.6
326*	G	-	108.5	-	47.5	-
327	N	-	130.2	173.3	51.8	38.9
328	I	-	122.1	174.4	60.0	40.4
329	H	-	125.4	174.2	55.8	30.0
330	H	-	125.4	174.4	55.8	30.0
331	K	-	121.3	-	54.9	37.3
332	P	-	-	174.8	63.5	32.5
333	G	8.6	116.3	170.5	46.3	-
334	G	7.2	101.6	174.0	43.8	-
335	G	7.8	101.6	172.8	44.8	-
336	Q	8.2	123.1	174.4	55.1	37.0
337	V	8.4	124.2	174.5	61.1	35.7
338	E	8.9	128.3	174.2	54.4	32.7
339	V	8.7	125.4	175.7	62.6	35.2

(: G326 is a tentative assignment)*

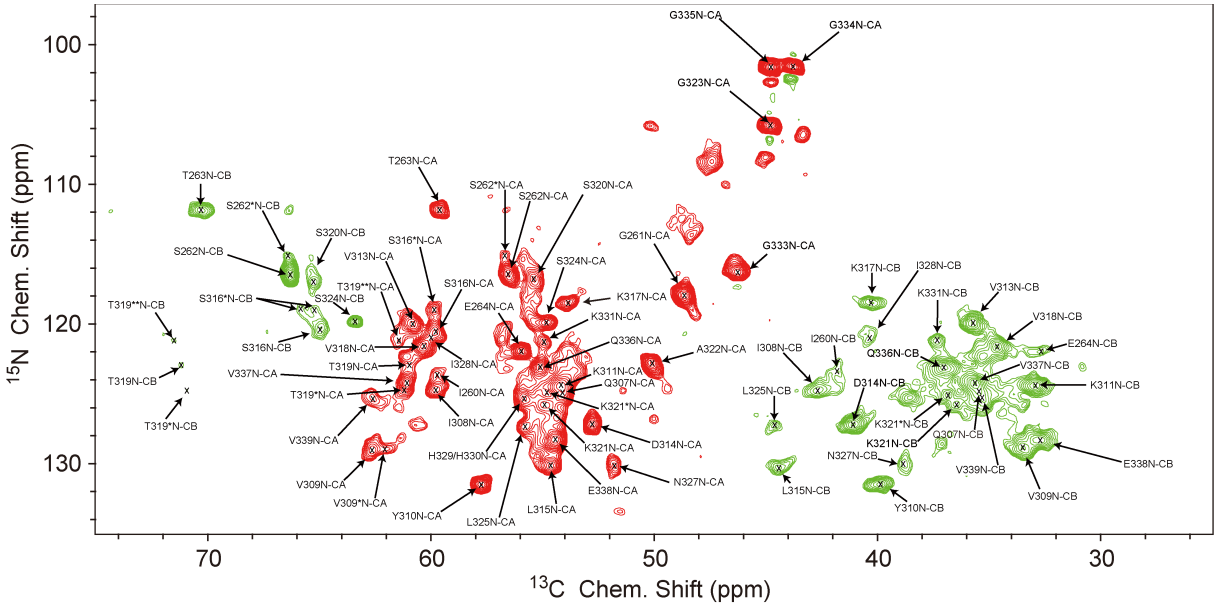

Fig. 3: 2D NCACB spectrum of sample D, recorded together with a high-resolution NCA (see main text Fig. 3) for ^{15}N linewidth extraction via the Bruker Topspin line shape analysis routine. A combination of NCB peaks with NCA peaks turned out to be useful for ^{15}N linewidths, since overlap found in the NCA is then mostly resolved. ^{15}N indirect evolution t_{1max} amounted to 18 ms in both cases. Experimental parameters are given on SI page 1.

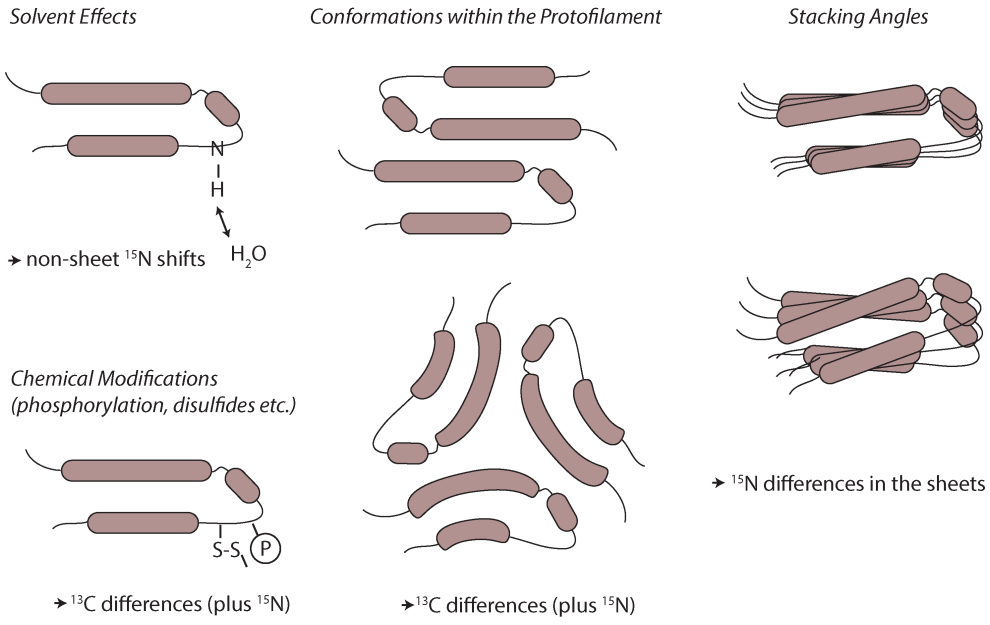

Fig. 4: Potential sources of chemical shift differences between preparations (selection) and the expected trends with respect to influences on solid-state NMR spectra. Note that the U-turn is a sketch and used only for the representation of potential structural variations of fibril polymorphism.

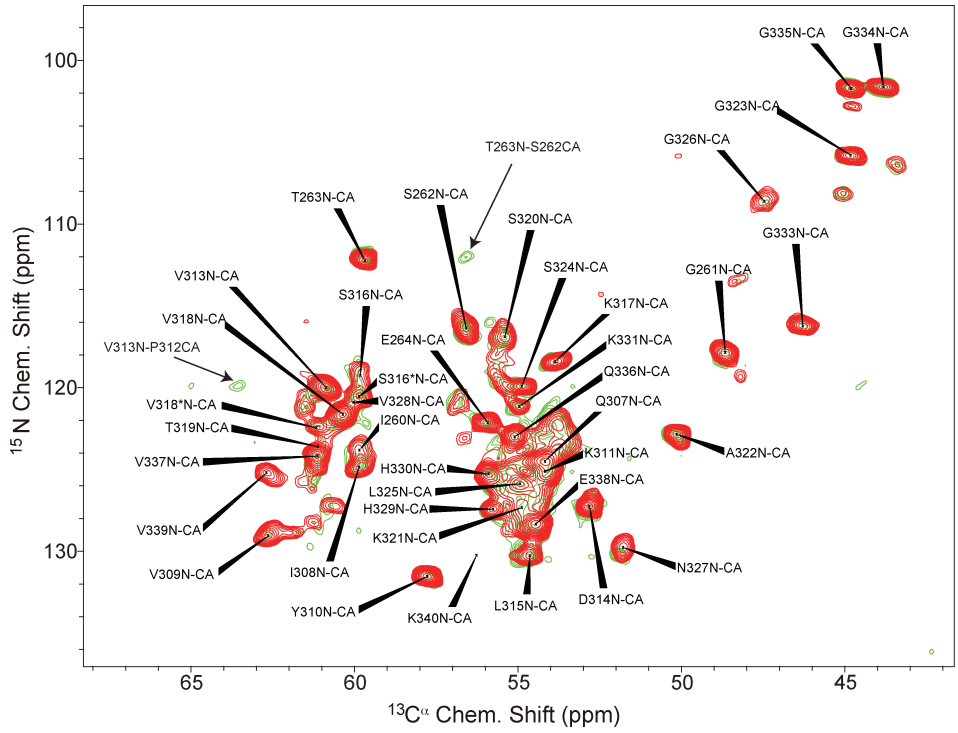

Fig. 5: Spectra of Tau PHFs (sample D) directly after their formation in 50 mM phosphate buffer (green), pH 6.8, and after extensive washes with pure water (red). Experimental parameters are given on SI page 1.

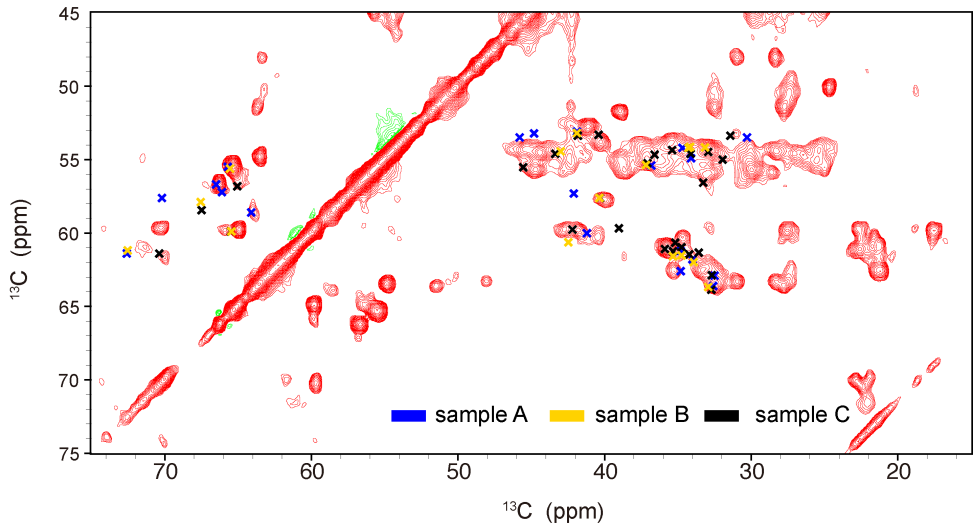

Fig. 6: Overlay of a ^{13}C-^{13}C correlation of latest (best resolved) sample (sample D) with positions of assigned peaks in earlier samples.

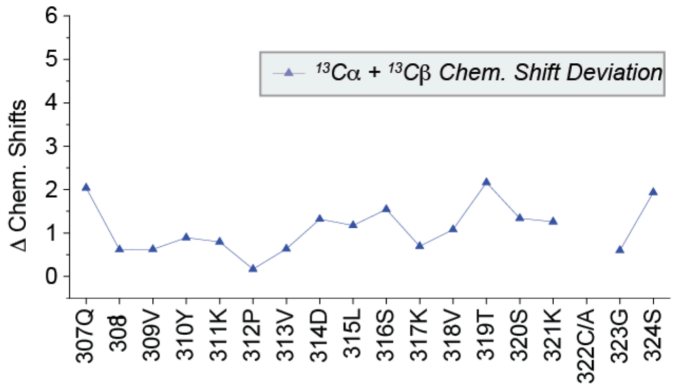

Fig. 7: Total combined deviation (RMSD) of the sum of aliphatic ^{13}C shifts (C^{α} + C^{β}) over four different preparations A, B, C, and D.

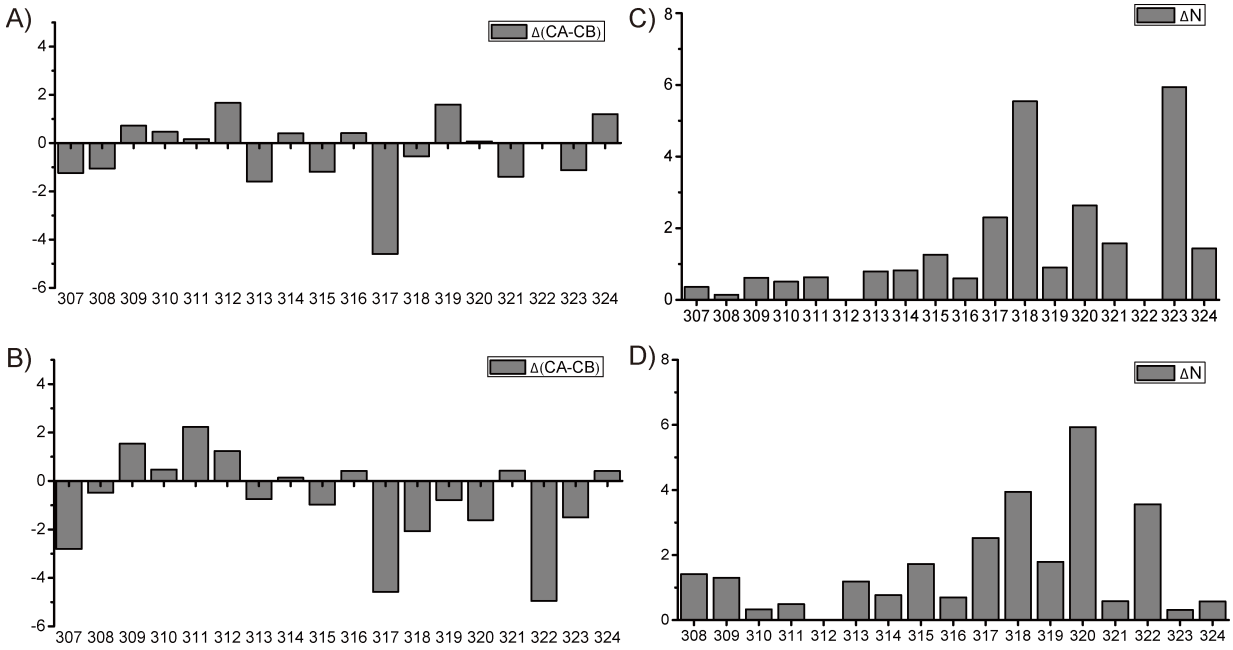

Fig. 8: Differences comparing pairs of preparations. Panels A) and B) show secondary chemical-shift differences: samples D vs. sample B (panel A), sample D vs. sample C (panel B). Panels C) and D) show ^{15}N chemical-shift differences: sample D vs. sample B (panel C), sample D vs. sample C (panel D).

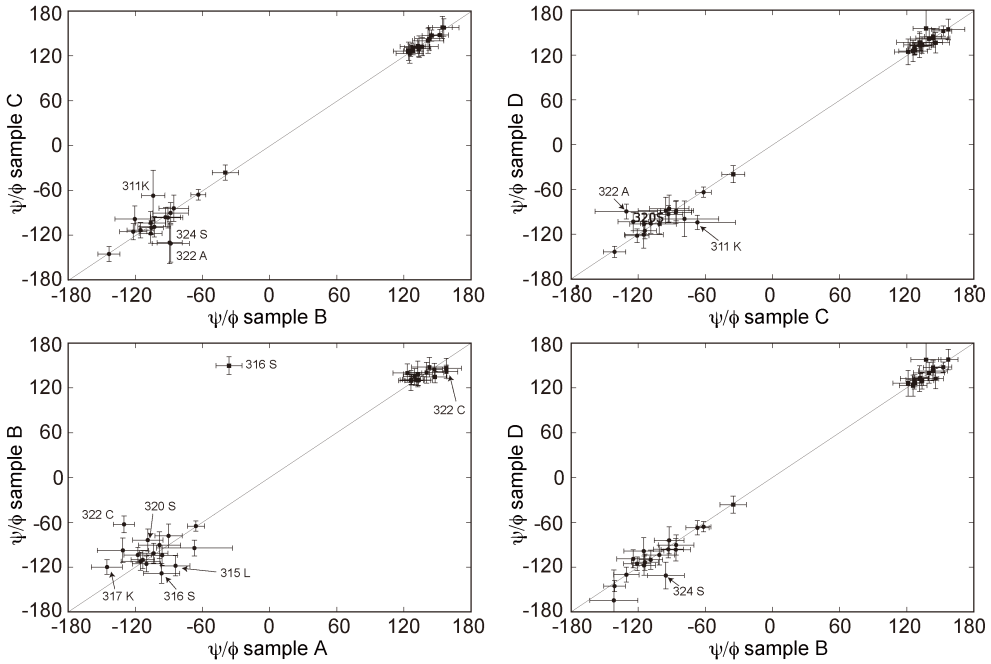

Fig. 9: Dihedral angle correlations between different pairs of samples. Upper left: comparison between samples B and C, upper right: comparison between samples C and D, lower left: comparison between samples A und B, and lower right: comparison between samples B and D. Negative angles reflect ϕ, positive angles ψ, except for S316 (marked in lower left plot).

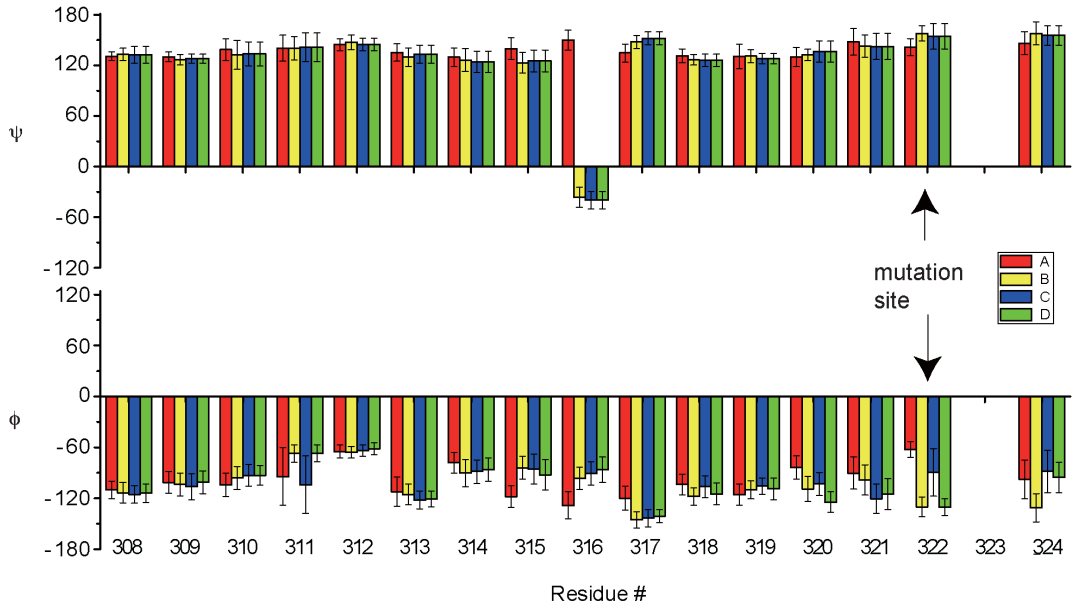

Fig. 10: Dihedral angles for samples A-D, as obtained from TALOS[10] predictions.

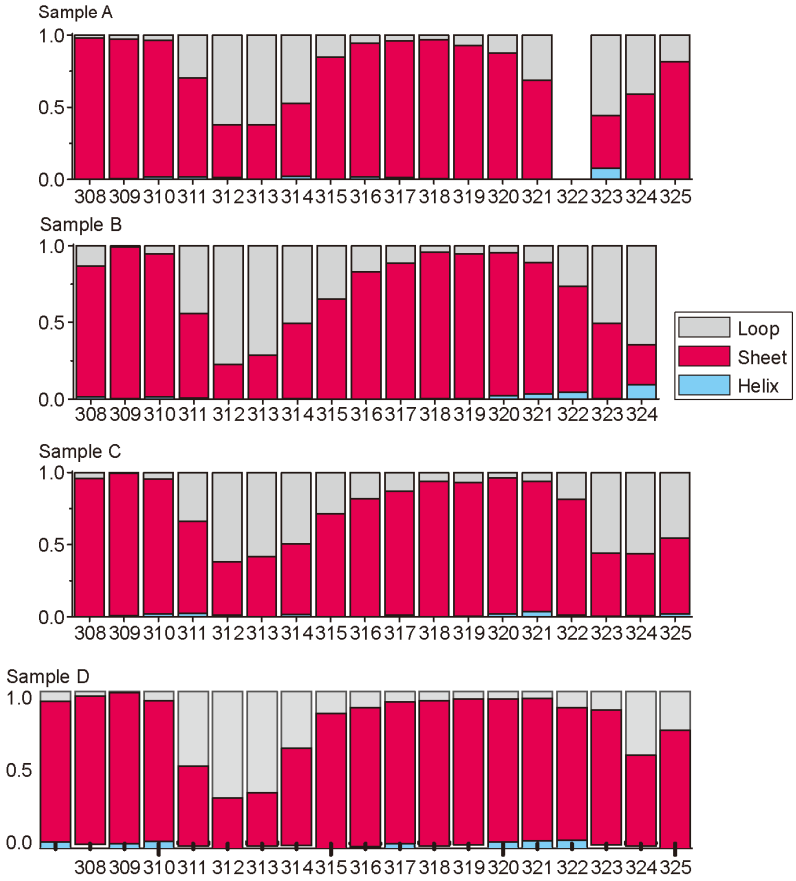

Fig. 11: Secondary structure propensities of those residues that are assigned in all samples A-D according to TALOS[10].

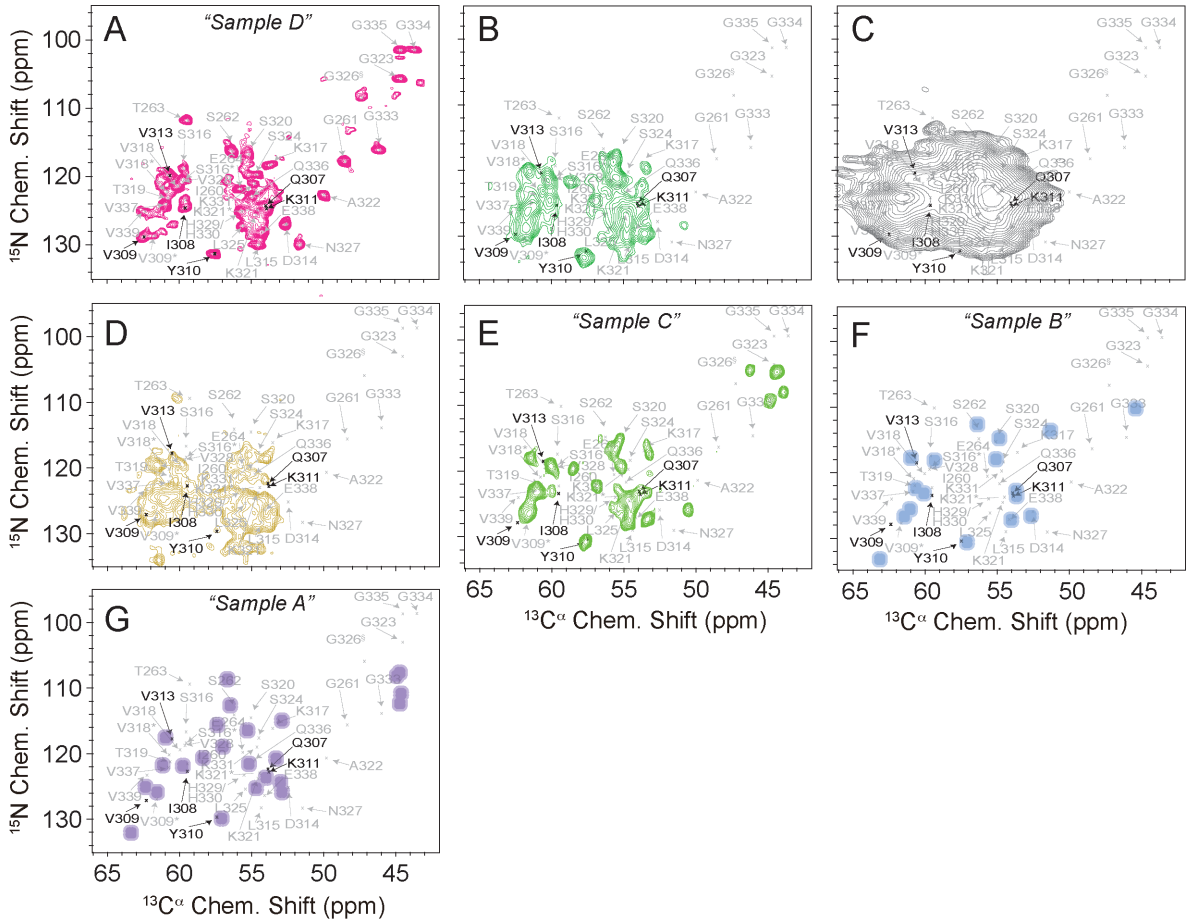

Fig. 12: Fingerprint spectra arising from different preparations. Despite variations of many residues' peaks, some residues (like the hexapeptide residues denoted in black writing) retain consistent shifts. A) Standard fibrilization protocol, most homogeneous sample (sample "D"). B) Fibrillization at a strongly decreased protein concentration (100 µM vs. 2.8 mM) with protein : heparin (MW ~20.000 Da (Roth)) ratio of 4:1. C) Protocol with sonication/seeding (see details below). D) Standard protocol with smaller-molecular-weight heparin (Mw ~5000 Da, Celsus). E) Sample preparation as in D), but with a different batch of heparin (sample "C"). F) Synthetic spectrum from shift lists obtained in Daebel et al.[9] (sample "B"). G) Synthetic spectrum from samples used in Andronesi et al.[1] (sample "A"). Gray/black crosses in A-G denote shifts as picked and assigned in sample D (panel A) for orientation. All spectra were recorded under similar conditions and identical temperatures using the same spectrometer, and aligned with respect to panel A. Apodization was applied as adequate for each spectrum obtained.

(Details for panel C) Use of a modified protocol.[11] The purified Tau protein was redissolved in a small volume of guanidinium hydrochloride to remove all aggregates and passed over a PD-10 desalting column to remove the denaturant before PHF assembly. Fibrillization was performed stepwise. Initially a small-scale PHF assembly was performed with 50 µM Tau : 12.5 µM heparin (MW ~5000 Da) for 3 days at 37 °C. From this aggregation 0.02 mol % Tau fibril seeds were added to another PHF assembly mixture with one-second sonication pulses (TT13, Bandelin, 10% intensity) immediately after addition of the seeds and five hours after seeding to generate as many seeds as possible. This seeding procedure was repeated two more times on small scale and finally seeds were transferred to a large scale PHF assembly mixture.)

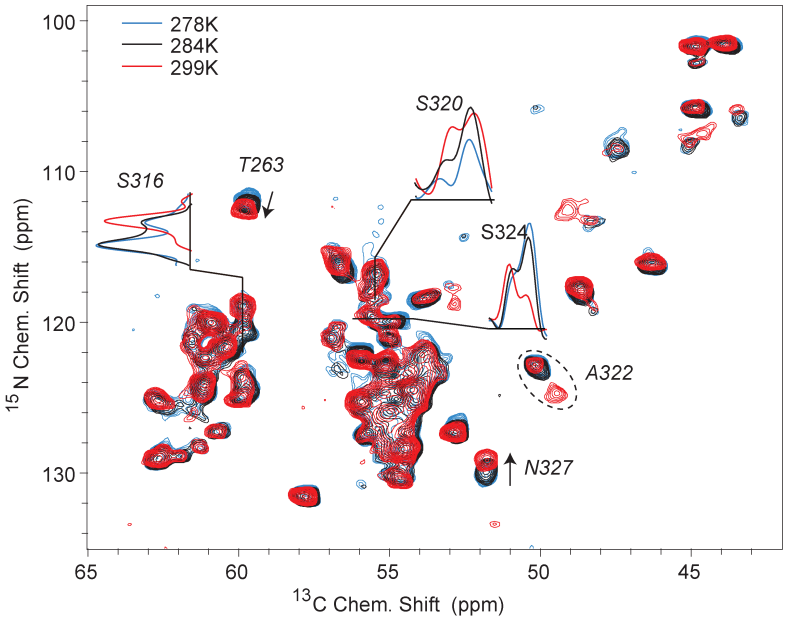

Fig. 13: Temperature dependence of Tau fibril (sample *D*) resonances. Some residues with strong temperature dependence (compare Fig. 3D of the main text) are highlighted in the figure. Cross sections for three Ser residues are shown as inserts in the figure to demonstrate the distribution of populations changing with temperature. Assignments were obtained from all available 3D and 4D experiments based on ^{13}C detection at low temperature or based on ^{1}H detection at high temperature, respectively. Experimental parameters are given on SI page 1. As opposed to proton shifts, ^{15}N shift temperature dependency does not directly reveal whether an amide is involved in a hydrogen bond or not.[12,13] It is, however, still expected to be different for those amides that are conformationally rigid compared with those that are susceptible for temperature-induced activation of dynamic modes. Apart from some (annotated) exceptions, no major shift changes are observed.

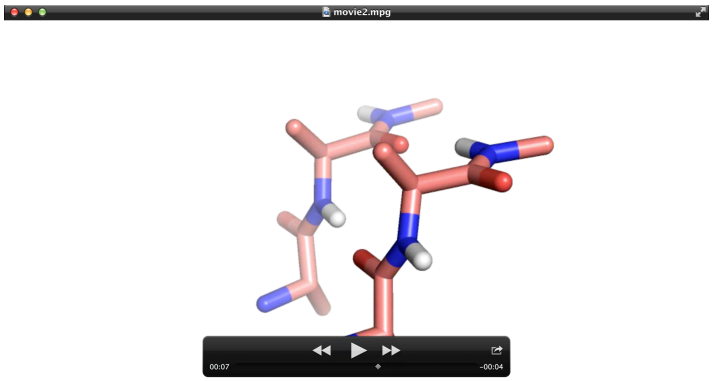

Supplementary Movie.
Animated representation of differences in Tau structure that would explain the NMR data obtained (see main text). Secondary structure of a given position in the sequence appears highly invariable between fibrils, as judged by TALOS[10]-predicted backbone dihedral angles. Variations in amide-bonded ^{15}N shifts, in conjunction with maintained secondary structure, may originate from differences in supramolecular arrangement (inter-monomer interactions) as the dominating kind of structural variability: Inhomogeneity in the amide bonds can again be due to translational variability (represented as dark green states), tilted strands (states shown in yellow), and twisting of strand with respect to another (red states). All of such beta-sheet structural variations are well known for intramolecular sheets. [14,15] PHF residues, by contrast, are of comparably low variance both in terms of secondary structure and regarding amide chemical environment/geometries (represented in blue).

References:

(1) Andronesi, O. C.; von Bergen, M.; Biernat, J.; Seidel, K.; Griesinger, C.; Mandelkow, E.; Baldus, M. *J. Am. Chem. Soc.* **2008**, *130*, 5922.

(2) Xiang, S.; Biernat, J.; Mandelkow, E.; Becker, S.; Linser, R. *ChemComm* **2016**, *52*, 4002.

(3) Xiang, S.; Chevelkov, V.; Becker, S.; Lange, A. *J. Biomol. NMR* **2014**, *60*, 85.

(4) Xiang, S.; Grohe, K.; Rovó, P.; Vasa, S.; Giller, K.; Becker, S.; Linser, R. *J. Biomol. NMR* **2015**, *62*, 303.

(5) Vranken, W. F.; Boucher, W.; Stevens, T. J.; Fogh, R. H.; Pajon, A.; Llinas, P.; Ulrich, E. L.; Markley, J. L.; Ionides, J.; Laue, E. D. *Proteins* **2005**, *59*, 687.

(6) Goddard, T. D.; Kneller, D. G. *SPARKY 3, University of California, San Francisco, CA*.

(7) Kumashiro, K. K.; Schmidt-Rohr, K.; Murphy III, O. J.; Ouellette, K. L.; Cramer, W. A.; Thompson, L. K. *J. Am. Chem. Soc.* **1998**, *120*, 5043.

(8) Chevelkov, V.; Shi, C.; Fasshuber, H. K.; Becker, S.; Lange, A. *J. Biomol. NMR* **2013**, *56*, 303.

(9) Daebel, V.; Chinnathambi, S.; Biernat, J.; Schwalbe, M.; Habenstein, B.; Loquet, A.; Akoury, E.; Tepper, K.; Müller, H.; Baldus, M.; Griesinger, C.; Zweckstetter, M.; Mandelkow, E.; Vijayan, V.; Lange, A. *J. Am. Chem. Soc.* **2012**, *134*, 13982.

(10) Shen, Y.; Delaglio, F.; Cornilescu, G.; Bax, A. *J. Biomol. NMR* **2009**, *44*, 213.

(11) Meyer, V.; Dinkel, P. D.; Rickman Hager, E.; Margittai, M. *Biochemistry* **2014**, *53*, 5804.

(12) Cierpicki, T.; Otlewski, J. *J. Biomol. NMR* **2001**, *21*, 249.

(13) Tomlinson, J. H.; Williamson, M. P. *J. Biomol. NMR* **2012**, *52*, 57.

(14) Weatherford, D. W.; Salemme, F. R. *Proc. Natl. Acad. Sci. U.S.A.* **1979**, *76*, 19.

(15) Salemme, F. R. *Prog. Biophys. Molec. Biol.* **1983**, *42*, 95.